



Published in final edited form as:

*J Am Chem Soc.* 2014 January 29; 136(4): 1174–1177. doi:10.1021/ja4091885.

## Direct EPR Observation of a Tyrosyl Radical in a Functional Oxidase Model in Myoglobin during both H<sub>2</sub>O<sub>2</sub> and O<sub>2</sub> Reactions

Yang Yu<sup>#†</sup>, Arnab Mukherjee<sup>#‡</sup>, Mark J. Nilges<sup>¶</sup>, Parisa Hosseinzadeh<sup>§</sup>, Kyle D. Miner<sup>§</sup>, and Yi Lu<sup>\*†‡§</sup>

<sup>†</sup>Center for Biophysics and Computational Biology, University of Illinois at Urbana–Champaign, Urbana, Illinois 61801, United States

<sup>‡</sup>Department of Chemistry, University of Illinois at Urbana–Champaign, Urbana, Illinois 61801, United States

<sup>§</sup>Department of Biochemistry, University of Illinois at Urbana–Champaign, Urbana, Illinois 61801, United States

<sup>¶</sup>The Illinois EPR Research Center, University of Illinois at Urbana–Champaign, Urbana, Illinois 61801, United States

<sup>#</sup> These authors contributed equally to this work.

### Abstract

Tyrosine is a conserved redox-active amino acid that plays important roles in heme-copper oxidases (HCO). Despite the widely proposed mechanism that involves a tyrosyl radical, its direct observation under O<sub>2</sub> reduction condition remains elusive. Using a functional oxidase model in myoglobin called F33Y-Cu<sub>B</sub>Mb that contains an engineered tyrosine, we report herein direct observation of a tyrosyl radical during both reactions of H<sub>2</sub>O<sub>2</sub> with oxidized protein and O<sub>2</sub> with reduced protein by electron paramagnetic resonance spectroscopy, providing a firm support of the tyrosyl radical in the HCO enzymatic mechanism.

As a redox active amino acid, tyrosine (Tyr) plays important roles in a number of enzymes.<sup>1-5</sup> Of particular interests is the Tyr in heme-copper oxidases.<sup>6-8</sup> In this class of proteins, O<sub>2</sub> is reduced to water at the binuclear heme-copper active site with a conserved Tyr next to one of the histidines that coordinate to the Cu<sub>B</sub> center. The Tyr is proposed to donate an electron and a proton in the reaction process, forming a radical intermediate.<sup>7-11</sup> To confirm the hypothesis, Babcock and coworkers have used radioactive iodine to label the tyrosyl radical in oxygen reduction reaction and mapped the radical to peptide corresponding to the active site tyrosine.<sup>12</sup> However, due to the transient nature of tyrosyl radical and P<sub>M</sub> intermediate associates with it, the tyrosyl radical has not been directly observed during the oxygen reduction reaction.<sup>5</sup> Instead, a number of groups have treated the oxidized HCOs with H<sub>2</sub>O<sub>2</sub>, and observed a radical formed in this process.<sup>13-18</sup> Recently, Gerfen and coworkers have performed high frequency EPR on H<sub>2</sub>O<sub>2</sub>-reacted bovine CcO and separated two tyrosyl radical signals, one of which is assigned to active site Tyr (Tyr244).<sup>19</sup> Even though the tyrosyl radical was observed under these “peroxide shunt”

\*Corresponding Author: yi-lu@illinois.edu.

Supporting Information

Experimental details, EPR of F33Y-Cu<sub>B</sub>Mb, Cu<sub>B</sub>Mb and WT Mb, spin counting, EPR parameters from simulation. This material is available free of charge via the Internet at <http://pubs.acs.org>.

The authors declare no competing financial interests.

pathway, direct observation of such a radical under physiological condition where  $O_2$  reduction occurred remains elusive; it is an important piece of the puzzle of the HCO reaction mechanism that is still missing.

One contributing factor in the lack of the proof of tyrosyl radical in  $O_2$  reduction in HCO is the difficulty in preparing and studying large membrane proteins such as HCO that contains several redox active centers that may interfere with spectroscopic characterizations. To overcome this limitation, synthetic models of HCOs have been prepared and they have contributed to understanding structure and function of HCO.<sup>20,21,22</sup> Phenoxyl radical has been generated in model complex by UV laser irradiation.<sup>22</sup> However, such a radical has not been observed as an intermediate in any  $O_2$  or  $H_2O_2$  reactions that are related to the biological function of HCO.<sup>20-24</sup>

As a complementary approach for studying native enzymes or synthetic models, we have previously reported designs of functional protein models of HCO by introducing one Tyr and three His into sperm whale myoglobin.<sup>25-34</sup> Interestingly, we found that the presence of a Tyr in the HCO protein model called F33Y-Cu<sub>B</sub>Mb (Figure 1) is critical in conferring the oxidase activity (turnover rate  $0.09\text{ s}^{-1}$  with  $258\text{ }\mu\text{M } O_2$  at  $25\text{ }^\circ\text{C}$  while native HCOs from different organisms display turnover rate in a range of  $50\text{-}1000\text{ s}^{-1}$  with respect to  $O_2$  consumption<sup>35,36</sup>) that reduces oxygen to water with minimal release of other reactive oxygen species such as superoxide and peroxide.<sup>30</sup> Here we report that such a functional protein model of HCO allows direct observation of a tyrosyl radical not only in the peroxide shunt pathway, but also during the  $O_2$  reduction, confirming active role of the tyrosyl radical in the oxidase reaction.

The F33Y-Cu<sub>B</sub>Mb was expressed and purified without a copper ion at the Cu<sub>B</sub> site, as previously described.<sup>30</sup> No copper ion was added in this work, as previous studies have shown the presence of copper does not have any influence on the oxidase activity,<sup>30</sup> similar to the Cu<sub>B</sub>-independent cytochrome *bd* oxidase.<sup>37-39</sup> The protein displays an EPR signal typical of water bounded high spin ferric myoglobin (Figure 2). Upon reaction with one equivalent of  $H_2O_2$  for 30 s when the reaction was stopped by flash freezing in liquid  $N_2$ , the high spin heme signal decreased by 80% and a  $g\approx 2$  signal grew in, accounting for 54% of the total protein concentration (Figure S1, Table S1). To further characterize the  $g\approx 2$  signal, an EPR spectrum was collected in this region using smaller modulation at 2 Gauss. Under such condition, an exquisite hyperfine structure was observed (Figure 3a), which is similar to that of tyrosyl radical reported in heme-copper oxidase<sup>14</sup> and ribonucleotide reductase.<sup>40-42</sup>

In addition to tyrosine, another redox active amino acid, tryptophan, could also generate a radical with a similar shape in X-band EPR as both wild type myoglobin (WTMb) and F33Y-Cu<sub>B</sub>Mb contain two Trp residues.<sup>2,40,43,44</sup> To improve the accuracy in EPR fitting, we collected Q-band EPR spectrum of a sample prepared in the same way (Figure 3b) and performed simulation<sup>45</sup> of both X- and Q-band spectra to extract *g*-values and hyperfine coupling constants (Tables 1 and S2). Simulation of both X- and Q-band spectra (Figures 3, S2, and S3) revealed two species. One species shows well-defined proton-hyperfine coupling pattern that can be simulated as a radical split by four nuclei, presumably from 3, 5-<sup>1</sup>H and two  $\beta$ -<sup>1</sup>Hs of a tyrosine. The other species has an unresolved hyperfine structure whose width and intensity vary with preparation such as tube size and mixing (Figure S2 and Table S2), in contrast to the first species. The width of the second species also differs from that of the radical formed in Cu<sub>B</sub>Mb. The *g* values of the first species obtained from simulations of both X- and Q-band EPR spectra are 2.0091, 2.0044 and 2.0021. This large *g* anisotropy is very similar to that of a typical tyrosyl radical (2.0091, 2.0046, 2.0021) and different from more isotropic values (2.0033, 2.0024, 2.0021) of a tryptophan radical

reported previously.<sup>40,42,46</sup> The hyperfine coupling constants of this species are also very similar to those of a tyrosyl radical from ribonucleotide reductase (RNR) from mouse (Table 1).<sup>40,42,46</sup> These similarities, especially for the more conserved hyperfine coupling constants of the ring protons,<sup>42,46,47</sup> also suggest the observed radical species is based on tyrosine. The yield of pure radical species is 29%, comparable to the yield of radical in HCOs (3-20%).<sup>13,14,19</sup>

In addition to engineered Tyr33, there are three other tyrosines (Tyr 103, 146 and 151) in the F33Y-Cu<sub>B</sub>Mb. To identify the location of the tyrosyl radical, we carried out several control experiments. First, under the same condition, reaction of 1 eq. of H<sub>2</sub>O<sub>2</sub> with WTMB, which contains the above three tyrosines but not Tyr33 resulted in no radical EPR signal in this region (Figure S4A and S4D). Second, the same reaction with Cu<sub>B</sub>Mb which contains the three tyrosines and the histidines for the Cu<sub>B</sub> site showed a broad signal with unresolved hyperfine structure (Figure S4B and S4E). Finally, when the three tyrosines in F33Y-Cu<sub>B</sub>Mb were mutated into Phe, the same reaction with H<sub>2</sub>O<sub>2</sub> under the same condition resulted in a radical signal that is almost identical to that without the above tyrosine mutations (Figure S5). Together these results indicate that the location of the radical with defined hyperfine coupling pattern (Figure 3) is at Tyr33. frequency: 9.23 GHz; power: 2 mW; gain: 4000; temperature: 30K; modulation: 2 Gauss. Experiment parameters for Q-band: frequency: 34.0 GHz; power: 50 μW; temperature: 50K; modulation: 3.2 Gauss. Spectrum simulated by SIMPOW6<sup>45</sup> was in red dashed line. Both temperature- (Figure S6) and microwave power- (Figure S7) dependent EPR studies indicate no spectral saturation occurred under the EPR condition used.

After demonstrating a protein radical, most probably formed on Tyr33, in the “peroxide shunt” pathway, we next investigate whether the Tyr radical can form during O<sub>2</sub> reduction reaction. Deoxy-F33Y-Cu<sub>B</sub>Mb was mixed with O<sub>2</sub> saturated buffer using a rapid freeze quench apparatus to trap reaction intermediate at ~20 ms. An EPR spectrum was then collected and compared with the corresponding EPR signal from oxidized protein (Fe(III)-F33Y-Cu<sub>B</sub>Mb) treated with H<sub>2</sub>O<sub>2</sub>. As shown in **Figure 4** and **Figure S8**, the radical signal of the freeze-quenched sample from direct O<sub>2</sub> reduction is similar to that from H<sub>2</sub>O<sub>2</sub> reaction, with similar hyperfine splitting pattern. The highly specific hyperfine splitting pattern suggests the same tyrosyl radical is generated through O<sub>2</sub> reduction reaction. The observed signal at the shortest time point (20 ms) of freeze quench represents ~ 7 % of total protein based on spin quantification (Table S1), and the signal intensity decreases further at 50 ms and disappears completely at 100 ms (Fig. S9), indicating that this tyrosyl radical is transient and unstable, consistent with difficulty in observing it in native HCOs under turnover conditions. Given the fast decay of the radical in comparison to the relatively slow turnover rate, the radical formation and decay is most likely not a rate determining step. Instead other steps, such as electron injection to the active site, may be limiting and will be investigated.

In summary, using EPR spectroscopy, we have detected the same radical species in the reaction of the ferric F33Y-Cu<sub>B</sub>Mb with H<sub>2</sub>O<sub>2</sub> and of the ferrous F33Y-Cu<sub>B</sub>Mb with O<sub>2</sub>. Simulation of the radical EPR spectra collected at both X- and Q-band showed it is consistent with a tyrosyl radical signal, while control experiments using WTMB, Cu<sub>B</sub>Mb and mutations of other native tyrosines in the protein established that Tyr33 is the active site Tyr involved in the radical formation. The direct observation of the tyrosyl radical in a functional oxidase model especially during O<sub>2</sub> reduction provides a strong support of the role of such radical in the oxidase reaction mechanism and thus fills an important missing piece in the puzzle of HCO bioenergetics.

## Supplementary Material

Refer to Web version on PubMed Central for supplementary material.

## Acknowledgments

We would like to thank Prof. Robert Gennis and Dr. Hanlin Ouyang, Ambika Bhagi and Shiliang Tian for helpful discussions. This report is based on work supported by the US National Institute of Health (GM062211).

## REFERENCES

1. Stubbe J, van der Donk WA. *Chem. Rev.* 1998; 98:705. [PubMed: 11848913]
2. Ivancich A, Dorlet P, Goodin DB, Un S. *J. Am. Chem. Soc.* 2001; 123:5050. [PubMed: 11457334]
3. Dempsey JL, Winkler JR, Gray HB. *Chem. Rev.* 2010; 110:7024. [PubMed: 21082865]
4. Warren JJ, Winkler JR, Gray HB. *FEBS Lett.* 2012; 586:596. [PubMed: 22210190]
5. Yu MA, Egawa T, Shinzawa-Itoh K, Yoshikawa S, Yeh S-R, Rousseau DL, Gerfen GJ. *Biochim. Biophys. Acta.* 2011; 1807:1295. [PubMed: 21718686]
6. Siegbahn PEM, Blomberg MRA. *Biochim. Biophys. Acta, Bioenerg.* 2004; 1655:45.
7. Hemp J, Gennis RB. *Results Probl. Cell Differ.* 2008; 45:1. [PubMed: 18183358]
8. Wikström M. *Biochim. Biophys. Acta.* 2012; 1817:468. [PubMed: 22079200]
9. Ostermeier C, Harrenga A, Ermler U, Michel H. *Proc. Natl. Acad. Sci. U. S. A.* 1997; 94:10547. [PubMed: 9380672]
10. Proshlyakov DA, Pressler MA, Babcock GT. *Proc. Natl. Acad. Sci. U. S. A.* 1998; 95:8020. [PubMed: 9653133]
11. Brzezinski P, Gennis RB. *J. Bioenerg. Biomembr.* 2008; 40:521. [PubMed: 18975062]
12. Proshlyakov DA, Pressler MA, DeMaso C, Leykam JF, DeWitt DL, Babcock GT. *Science.* 2000; 290:1588. [PubMed: 11090359]
13. Fabian M, Palmer G. *Biochemistry.* 1995; 34:13802. [PubMed: 7577973]
14. MacMillan F, Kannt A, Behr J, Prisner T, Michel H. *Biochemistry.* 1999; 38:9179. [PubMed: 10413492]
15. Rigby SE, Junemann S, Rich PR, Heathcote P. *Biochemistry.* 2000; 39:5921. [PubMed: 10821663]
16. Rich PR, Rigby SE, Heathcote P. *Biochim. Biophys. Acta.* 2002; 1554:137. [PubMed: 12160986]
17. Budiman K, Kannt A, Lyubenova S, Richter OM, Ludwig B, Michel H, MacMillan F. *Biochemistry.* 2004; 43:11709. [PubMed: 15362855]
18. Svistunenko DA, Wilson MT, Cooper CE. *Biochim. Biophys. Acta, Bioenerg.* 2004; 1655:372.
19. Yu MA, Egawa T, Shinzawa-Itoh K, Yoshikawa S, Guallar V, Yeh S-R, Rousseau DL, Gerfen GJ. *J. Am. Chem. Soc.* 2012; 134:4753. [PubMed: 22296274]
20. Kim E, Chufán EE, Kamaraj K, Karlin KD. *Chem. Rev.* 2004; 104:1077. [PubMed: 14871150]
21. Collman JP, Devaraj NK, Decréau R, Yang Y, Yan Y-L, Ebina W, Eberspacher T, Chidsey CED. *Science.* 2007; 315:1565. [PubMed: 17363671]
22. Nagano Y, Liu J-G, Naruta Y, Ikoma T, Tero-Kubota S, Kitagawa TJ. *Am. Chem. Soc.* 2006; 128:14560.
23. Halime Z, Kotani H, Li Y, Fukuzumi S, Karlin KD. *Proc. Natl. Acad. Sci. U. S. A.* 2011; 108:13990. [PubMed: 21808032]
24. Liu J-G, Naruta Y. *Indian J. Chem., Sect. A: Inorg., Bio-inorg., Phys., Theor. Anal. Chem.* 2011; 50:363.
25. Sigman, J. a.; Kwok, BC.; Lu, Y. *J. Am. Chem. Soc.* 2000; 122:8192.
26. Sigman, J. a.; Kim, HK.; Zhao, X.; Carey, JR.; Lu, Y. *Proc. Natl. Acad. Sci. U. S. A.* 2003; 100:3629. [PubMed: 12655052]
27. Wang N, Zhao X, Lu YJ. *Am. Chem. Soc.* 2005; 127:16541.
28. Zhao X, Nilges MJ, Lu Y. *Biochemistry.* 2005; 44:6559. [PubMed: 15850389]
29. Zhao X, Yeung N, Wang Z, Guo Z, Lu Y. *Biochemistry.* 2005; 44:1210. [PubMed: 15667214]

30. Miner KD, Mukherjee A, Gao Y-G, Null EL, Petrik ID, Zhao X, Yeung N, Robinson H, Lu Y. *Angew. Chem., Int. Ed.* 2012; 51:5589.
31. Liu X, Yu Y, Hu C, Zhang W, Lu Y, Wang J. *Angew. Chem., Int. Ed.* 2012; 51:4312.
32. Lu Y. *Angew. Chem., Int. Ed.* 2006; 45:5588.
33. Yeung N, Lin Y-W, Gao Y-G, Zhao X, Russell BS, Lei L, Miner KD, Robinson H, Lu Y. *Nature.* 2009; 462:1079. [PubMed: 19940850]
34. Lu, Y.; Chakraborty, S.; Miner, KD.; Wilson, TD.; Mukherjee, A.; Yu, Y.; Liu, J.; Marshall, NM. In *Comprehensive Inorganic Chemistry II. Second Edition.* Reedijk, J.; Poeppelemeier, K., editors. Elsevier; Amsterdam: 2013. p. 565
35. Pawate AS, Morgan J, Namslauer A, Mills D, Brzezinski P, Ferguson-Miller S, Gennis RB. *Biochemistry.* 2002; 41:13417. [PubMed: 12416987]
36. Lee HJ, Gennis RB, Adelloth P. *Proc. Natl. Acad. Sci. U. S. A.* 2011; 108:17661. [PubMed: 21997215]
37. Hill JJ, Alben JO, Gennis RB. *Proc. Natl. Acad. Sci. U. S. A.* 1993; 90:5863. [PubMed: 8516338]
38. Jünemann S. *Biochim. Biophys. Acta, Bioenerg.* 1997; 1321:107.
39. Borisov VB, Gennis RB, Hemp J, Verkhovsky MI. *Biochim. Biophys. Acta, Bioenerg.* 2011; 1807:1398.
40. Bleifuss G, Kolberg M, Pötsch S, Hofbauer W, Bittl R, Lubitz W, Gräslund A, Lassmann G, Lendzian F. *Biochemistry.* 2001; 40:15362. [PubMed: 11735419]
41. Seyedsayamdost MR, Stubbe JJ. *Am. Chem. Soc.* 2006; 128:2522.
42. Yokoyama K, Smith A. a. Corzilius B, Griffin RG, Stubbe J. *J. Am. Chem. Soc.* 2011; 133:18420. [PubMed: 21967342]
43. Di Bilio AJ, Crane BR, Wehbi WA, Kiser CN, Abu-Omar MM, Carlos RM, Richards JH, Winkler JR, Gray HB. *J. Am. Chem. Soc.* 2001; 123:3181. [PubMed: 11457048]
44. Shafaat HS, Leigh BS, Tauber MJ, Kim JE. *J. Am. Chem. Soc.* 2010; 132:9030. [PubMed: 20536238]
45. Nilges, MJ.; Matteson, K.; Bedford, RL. In *ESR Spectroscopy in Membrane Biophysics.* Hemminga, MA.; Berliner, L., editors. Vol. 27. Springer; New York: 2007.
46. Svistunenko DA, Cooper CE. *Biophys. J.* 2004; 87:582. [PubMed: 15240491]
47. Hoganson CW, Babcock GT. *Biochemistry.* 1992; 31:11874. [PubMed: 1332777]

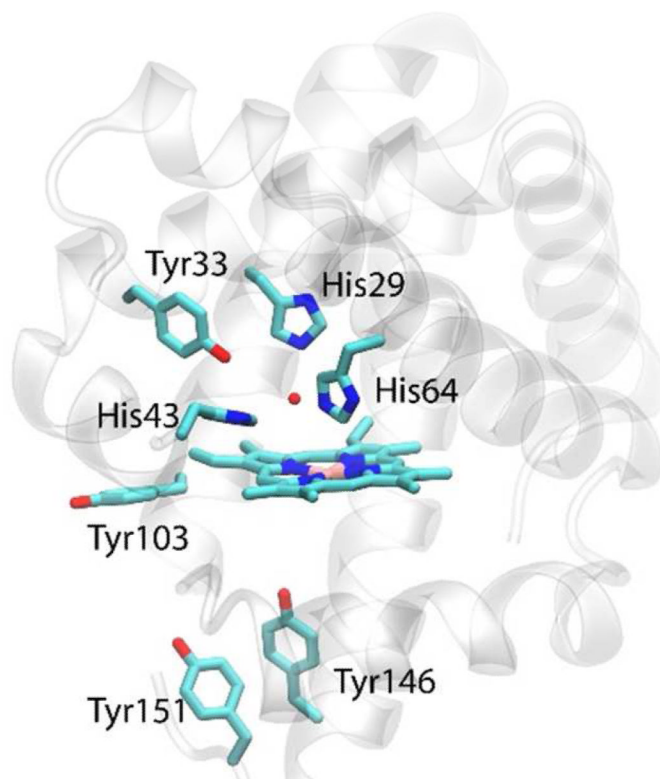


**Figure 1.** X-ray crystal structure of F33Y-Cu<sub>B</sub>Mb. Heme *b* and side chains of His29, His43, His64 and Tyr33 in Cu<sub>B</sub> site, as well as Tyr103, Tyr146 and Tyr151 were shown in licorice diagram. A water molecule, shown in red sphere, is present at the Cu<sub>B</sub> site. For the purpose of clarity, propionate side chains of heme were omitted. PDB ID: 4FWX.<sup>30</sup>

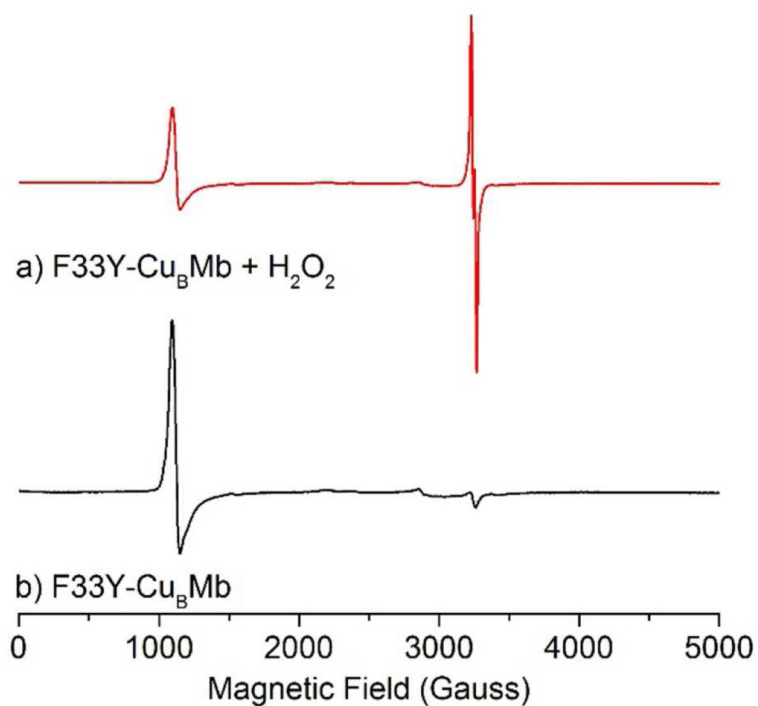


**Figure 2.** X-band EPR spectra of 0.2 mM F33Y-Cu<sub>B</sub>Mb in the absence (black line) and in the presence of (red line) 1 eq. of H<sub>2</sub>O<sub>2</sub> in 100 mM potassium phosphate buffer. Experiment parameters: frequency: 9.05 GHz; power: 5 mW; gain: 2000; temperature: 30K; modulation: 10 Gauss.

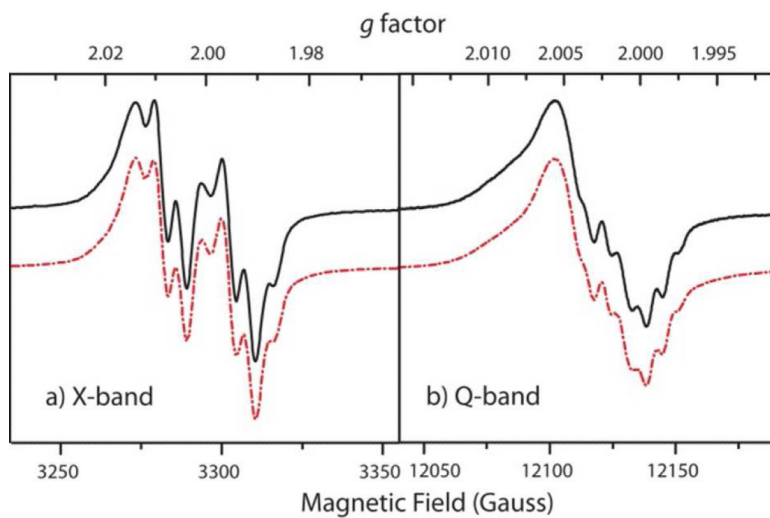


**Figure 3.** X-band (a) and Q-band (b) EPR spectra of F33Y-Cu<sub>B</sub>Mb after H<sub>2</sub>O<sub>2</sub> treatment. Experiment parameters for X-band:



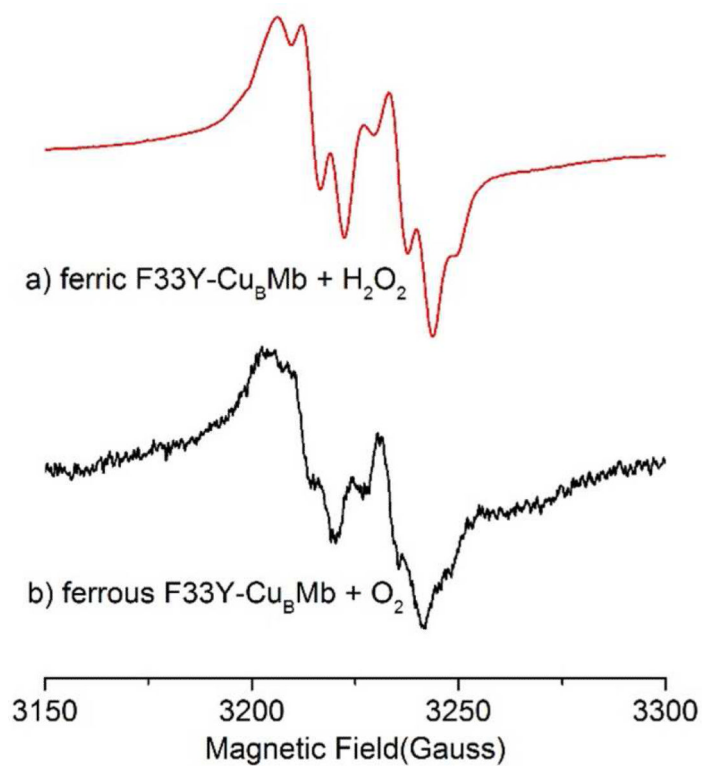


**Figure 4.** EPR spectra of ferric F33Y-Cu<sub>B</sub>Mb reacted with 1 eq of H<sub>2</sub>O<sub>2</sub> (a) and ferrous F33Y-Cu<sub>B</sub>Mb with O<sub>2</sub> (b). Ferrous F33Y-Cu<sub>B</sub>Mb was mixed with O<sub>2</sub> saturated buffer and rapid freeze-quenched to capture reaction intermediate. Experiment parameters for X-band EPR: frequency: 9.04 GHz; power: 2 mW; gain: 4000 for H<sub>2</sub>O<sub>2</sub>-reacted and 12500 for O<sub>2</sub>-reacted sample; temperature: 30K; modulation: 4 Gauss.

**Table 1**Simulated EPR parameters for tyrosyl radical in F33Y-Cu<sub>B</sub> Mb and RNR

	Nucleus	A <sub>x</sub> /MHz <sup>e</sup>	A <sub>y</sub> /MHz <sup>e</sup>	A <sub>z</sub> /MHz
F33Y-Cu <sub>B</sub> Mb <sup>a,b,c</sup>	3- <sup>1</sup> H <sup>d</sup>	26	11	19
	5- <sup>1</sup> H <sup>d</sup>	26	11	19
	β- <sup>1</sup> H	51	60	59
	β- <sup>1</sup> H	24	8	16
RNR <sup>f,g,h</sup>	3- <sup>1</sup> H	25	12	19
	5- <sup>1</sup> H	21	14	16
	β- <sup>1</sup> H	60	53	60
	β- <sup>1</sup> H	27	7	16

<sup>a</sup> *g* values of 2.0091, 2.0044 and 2.0021 were used.

<sup>b</sup> Line width (peak-to-peak) of 7.5, 4.7, 3.2 Gauss were used.

<sup>c</sup> *g* strain of 0.0005, 0.0001 and 0.0000 were used.

<sup>d</sup> Euler angle of [α,β,γ] = [±22°,0°,0°]<sup>46</sup> were used. Hyperfine for 3-H and 5-H assumed equivalent. No significant improvement if they are allowed to be inequivalent.

<sup>e</sup> The assignment of x versus y is arbitrary.

<sup>f</sup> from ref<sup>40</sup>.

<sup>g</sup> *g* values of 2.0076, 2.0044 and 2.0021 were used.

<sup>h</sup> Line widths of 6.0, 6.0, 6.0 Gauss were used.